Optical Experimental Evidence for a Universal Length Scale for the Dynamic Charge Inhomogeneity of Cuprate Superconductors

D. Mihailovic

Jozef Stefan Institute, Jamova 39, 1000 Ljubljana, Slovenia

(Received 12 August 2004; published 23 May 2005)

Time-resolved optical experiments can give unique information on the characteristic length scales of dynamic charge inhomogeneity on femtosecond time scales. From data on the effective quasiparticle relaxation time τ_r in $La_{2-x}Sr_xCuO_4$ and $Nd_{2-x}Ce_xCuO_4$, we derive the temperature and doping dependence of the intrinsic phonon escape length l_e, which can be a direct measure of charge inhomogeneity. Remarkably, a common feature of both p- and n-type cuprates is that, as $T \to T_c$, $l_e$approaches the superconducting coherence length $l_e \to \xi_s(0)$. In the normal state l_e is found to be in excellent agreement with the mean free path l_m obtained from the resistivity data and structural coherence lengths l_s from neutron scattering experiments, implying the existence of complex intrinsic textures on different length scales which may have a profound effect on the functional properties of these materials.

DOI: 10.1103/PhysRevLett.94.207001 PACS numbers: 74.25.Dw, 74.25.Jb, 78.47.+p

In recent years, substantial experimental evidence has started to accumulate for the existence of inhomogeneity in cuprates and other functional oxides, suggesting that it plays a fundamental role in their physics. Unfortunately, *dynamic* inhomogeneity—which is particularly important—is not easily and unambiguously detectable [1]. The current evidence for dynamic structural inhomogeneity comes from x-ray absorption fine structure spectroscopy [2] and neutron parton distribution function [3] experiments, which have sufficiently short intrinsic experimental time scales to give information on dynamical local structure fluctuations but unfortunately have a limited range of, at most, a few lattice constants [4]. Some other experiments, such as inelastic neutron scattering [5–7] and scanning tunneling microscopy [8], have suggested a characteristic length scale of the inhomogeneity of the order of 1–2 nm, but no information on the dynamics can be deduced from these experiments.

In this Letter, we present new femtosecond time scale information on charge inhomogeneity as a function of temperature and doping in selected cuprate superconductors. Using time-resolved optical experiments, we extract the characteristic length scale l_e of charge inhomogeneities from the effective quasiparticle lifetime τ_r, and compare these results to data obtained from other established techniques. We find remarkable agreement of the dynamical length scale measured by time-resolved spectroscopy with structural coherence lengths l_s determined from inelastic diffuse neutron scattering as well as the normal state mean free path l_m obtained from conductivity measurements.

To understand how we can derive a length scale from time-resolved measurements of the quasiparticle lifetimes, let us first consider the dynamics of the creation of bound states such as Cooper pairs (or charged stripes) from unbound particles. The formation of a bound state from unbound fermions leads to the release of energy 2Δ in the form of a phonon (there is no other excitation which can remove the energy from the electronic subsystem). However, as was pointed out by Rothwarf and Taylor (RT) already in 1967 [9], unless the phonon lifetime is zero, the emitted phonon can be efficiently reabsorbed again, breaking pairs and leading to the formation of a relaxation bottleneck. The overall kinetics of pairing is typically described by the RT rate equations for the quasiparticle density n and the optical phonon density N, respectively, as $\frac{dn}{dt} = I_0 + \beta N - Rn^2$ and $\frac{dN}{dt} = -\frac{1}{2}(\beta N - Rn^2) - \gamma(N - N_T)$, where β is the pair-breaking rate by phonons with $\hbar\omega_{\rm ph} > 2\Delta$, R is the recombination rate, N is the nonequilibrium density, and N_T is the density of optical phonons in thermal equilibrium. γ is the rate at which optical phonons decay or escape by processes other than pair excitation. Under bottleneck conditions, $\beta N \approx Rn^2$, and the overall relaxation rate is dominated by the phonon escape term $\gamma(N - N_T)$. Thus, the experimentally observed relaxation time τ_r is determined by the escape of phonons from the recombination volume rather than by the direct pair recombination rate R. In low-T_c superconductors which have a relatively small superconducting energy gap $2\Delta < 10$ meV, acoustic phonons are emitted by this process, and experiments on Al and Pb have clearly shown that the observed recombination time τ_r depends on superconducting film thickness, as predicted by the RT model [10].

In high-temperature superconductors, preformed pairs or other forms of bound states may form in the normal state ($T > T_c$), so RT relaxation might be expected also above T_c, where it would apply to the formation of bipolarons or stripes from unbound particles. First, high frequency optical phonons (with $\hbar\omega > 2\Delta$) are emitted, which subsequently decay anharmonically to acoustic phonons [11]. However, these acoustic phonons can efficiently recombine again to excite optical phonons, which in turn break up pairs again until eventually the acoustic phonons disperse out of the recombination volume. By analogy with the RT equations, the rate equations for the optical phonon

decay to acoustic phonons and acoustic phonon escape can then be written as

$$\frac{dN}{dt} = G_0 - \frac{1}{2}(\chi N - \delta M^2), \quad (1)$$

$$\frac{dM}{dt} = \chi N - \delta M^2 - \kappa(M - M_T), \quad (2)$$

where G_0 is the optical phonon generation rate by quasiparticles, M is the density of acoustic phonons, and $\kappa(M - M_T)$ describes the acoustic phonon escape; χ is the rate of optical phonon decay to acoustical phonons, while δ is the rate of acoustic phonon reabsorption. Under bottleneck conditions (i.e., near-steady-state) $\chi N \approx \delta M^2$; so using $\frac{dM}{dt} = \nu_s \frac{dM}{dr}$ [Eq. (2)], we obtain an explicit equation for the phonon escape:

$$\frac{dM}{dr} = -l_e^{-1}(M - M_T), \quad (3)$$

where $l_e = \nu_s/\kappa$ is the phonon escape length. The justification for the steady-state assumption can be tested through comparison with experiments. If it can be shown that l_e is determined by geometrical constraints, such as film thickness, as was done in conventional superconductors, then the bottleneck assumption can be fully justified. Importantly, if the material is intrinsically inhomogeneous, the relevant geometrical constraints on the recombination volume are determined by the inhomogeneity length scale, and the relaxation time may be dominated by the phonons' escape from one phase (charge rich) into another (charge poor), as shown schematically in the inset of Fig. 1. Inhomogeneities on the nanometer scale give rise to phonon escape times on the picosecond time scale, which is directly measurable with current ultrafast laser spectroscopy.

Over the past few years, several experiments have been carried out on cuprates to measure the temperature dependence of the relaxation time τ_r [11–17]. A typical data set showing the photoinduced normalized reflectivity as a function of time is shown in Fig. 1 for $La_{2-x}Sr_xCuO_4$, at different temperatures for $x = 0.1$. (The experimental details are described in Ref. [18].) From the fitted relaxation time τ_r, we can analyze the characteristic phonon escape lengths l_e as a function of T. We concentrate on $La_{2-x}Sr_xCuO_4$ (LSCO) here, because the relevant data are most complete for this compound. Using measured values of τ_r [18] and ν_s [19], in Fig. 2 we have plotted l_e for $x = 0.06$–0.2, at different temperatures. For all superconducting samples ($x = 0.1$–0.2), l_e shows a gradual increase from approximately $l_e \approx 1$ nm at 300 K to about $l_e \approx 2$–3 nm near T_c. Well below T_c, l_e continues to increase rapidly, but with a different slope. [On the other hand, the insulating sample ($x = 0.06$) shows almost no temperature dependence of l_e over this temperature range.]

Close to T_c, l_e shows signs of critical behavior, exhibiting a clear peak. This peak is more pronounced in some materials than in others [11–13,18] and depends on experimental conditions (such as incident laser power), but it is

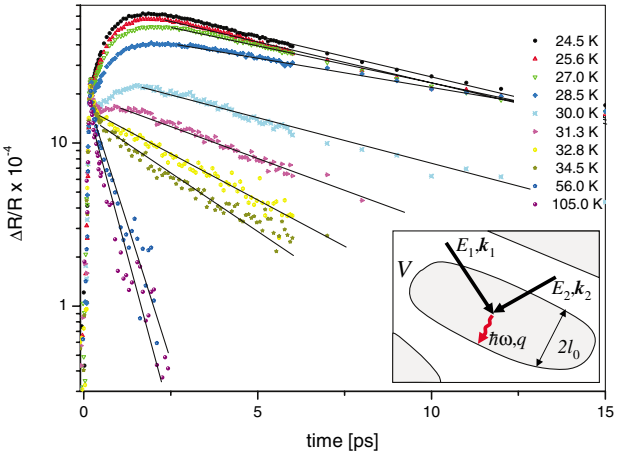

FIG. 1 (color). The photoinduced reflectivity $\Delta R/R$ measured on $La_{1.9}Sr_{0.1}CuO_4$ as a function of time for different T. The relaxation is described reasonably well by a single exponential. Inset: a schematic representation of the phonon escape process arising from the pairing of two particles with E_1, k_1 and E_2, k_2 (solid lines) with the emission of acoustic phonons (wavy line) in an inhomogeneous medium. The overall rate of recombination is dominated by phonon escape out of the charged volume V.

generally present only in a narrow 2–3 K region near T_c. At a second order phase transition (such as the superconducting transition), the correlation (coherence) length is expected to diverge as $\xi_s \sim (T_c - T)^{-\nu}$ above T_c and as $\xi_s \sim (T - T_c)^{-\nu}$ below T_c. Plotting the critical region near T_c for $La_{1.9}Sr_{0.1}CuO_4$ in the inset of Fig. 3(a), we see that the critical exponent of l_e is near $\nu = 0.5$, the mean-field theory value, and is consistent with the relation $l_e = v_s\tau_r \sim \Delta^{-1} \sim \xi_s^{-1/2}$ discussed previously [13]. The obvious implication from the data in Fig. 3(a), that l_e is related to $\xi_s(T)$ in the vicinity of T_c, is quite remarkable and is far from trivial. Although the detailed theoretical justification for this statement is beyond the scope of this Letter, we wish to remark here that the connection between $\xi_s(T)$ and

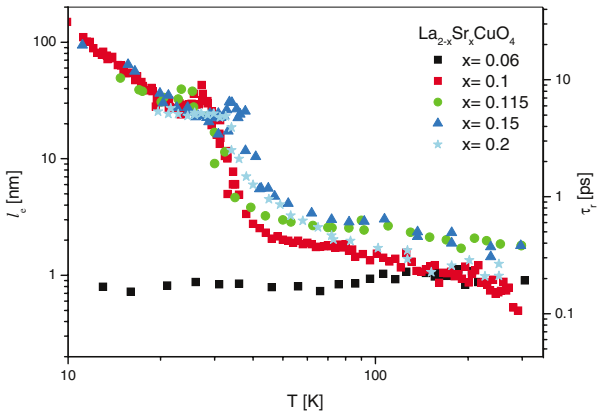

FIG. 2 (color). The phonon escape length l_e as a function of temperature for $La_{2-x}Sr_xCuO_4$ for $x = 0.06$, 0.1, 0.115, 0.15, and 0.2, respectively. The T_c are 0, 31, 32, 38, 5, and 30 K, respectively. ($x = 0.06$ is nonsuperconducting.) Here we have used $v_s = 4.8$ nm ps^{-1} for all x in LSCO [19].

$l_e(T)$ implies that the charge inhomogeneity governs the behavior of the superconducting phase coherence and the transition to the superconducting state at T_c [20]. The corollary is that the presence of inhomogeneity on a scale shorter than the coherence length clearly prevents the formation of a phase-coherent superconducting state.

We can check if our understanding of the recombination dynamics in terms of inhomogeneity-limited phonon escape is appropriate by comparing l_e with the length scales obtained from other experiments which can sense dynamic inhomogeneity, such as the mean free path l_m of charge carriers in the normal state. Expressing l_m via the Drude formula in terms of the relevant experimentally measurable quantities such as the ab-plane superconducting penetration depth λ_s and Fermi velocity ν_F (rather than effective mass and density), we obtain $l_m = (\lambda_s{}^2 \nu_F / \varepsilon_0 c^2)\sigma(T)$, where $\sigma(T)$ is the normal state conductivity. In Fig. 3(a) we show a comparison between l_e and l_m (normalized to ξ_s) using measured values of λ_s [21], ν_F [22], and in-plane $\sigma(T)$ [23] for $x = 0.1$ and $x = 0.15$ as a function of T/T_c. We observe remarkable quantitative agreement between l_e and l_m over the entire temperature range ($T_c < T < 300$ K) where the data sets overlap. The implication is that the charged carrier mean free path l_m and the phonon escape length l_e are both being determined by the same underlying texture, and, empirically, $\frac{\sigma(T)}{\tau_r(T)} \approx \varepsilon_0 c^2 \nu_s / \lambda_s{}^2 \nu_F$.

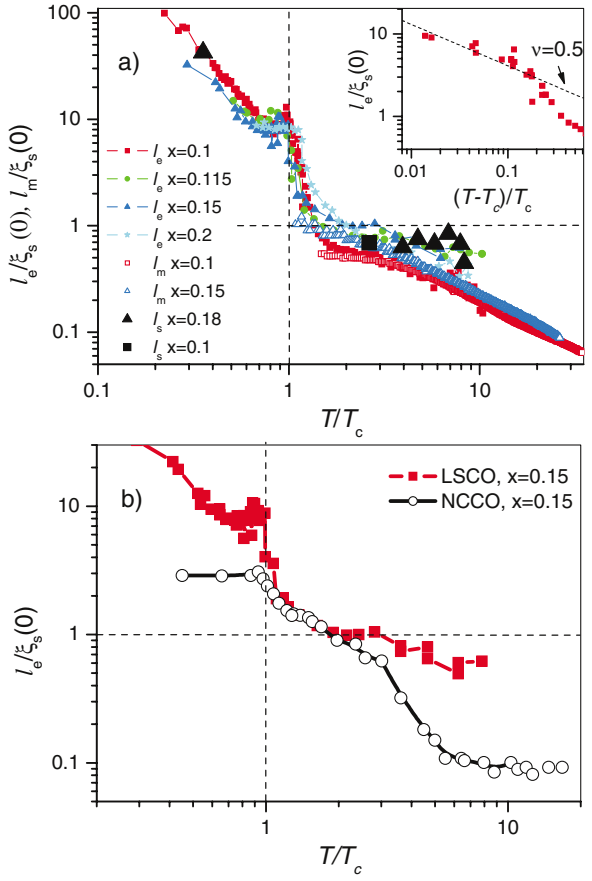

FIG. 3 (color). (a) A plot of l_e (solid color symbols), l_m (open symbols), and l_s (black symbols), as a function of T/T_c for LSCO at different doping levels. In all cases, the length scale is normalized to $\xi_s(0)$ [29]. The inset shows the critical behavior just above T_c for $x = 0.1$. The mean-field prediction is plotted $l/\xi_{GL}(T) \sim (T - T_c)^{-\nu}$, with $\nu = 1/2$ as a dashed line. (b) The normalized escape lengths $l_e/\xi_s(0)$ for $La_{1.85}Sr_{0.15}CuO_4$ (solid squares) and $Nd_{1.85}Ce_{0.15}CuO_4$ (open circles) as a function of T/T_c. Here $\xi_s(0) = 1.8$ and 18 nm, respectively, for LSCO and NCCO [24]. $v_s = 5.5$ nm ps^{-1} for NCCO [30].

To determine if the underlying length scale is connected with *structural* inhomogeneity, we compare l_m and l_e with the *structural* coherence length l_s determined by neutron scattering experiments on LSCO. The latter is defined as the length scale over which a particular structure that gives rise to the diffraction peak is coherent [7]. Although we are not aware of any detailed studies of structural inhomogeneities over a large range of temperature, Kimura *et al.* [7] deduced a structural coherence length of $l_s = 1/\Delta k \sim 1.7$ nm in slightly underdoped $La_{1.88}Sr_{0.12}CuO_4$ around 315 K from the linewidth of the diffuse central peak ($\Delta k = 0.06$ Å^{-1}) in neutron scattering. Well below T_c (at $T = 13.5$ K), this structural coherence length is apparently extended to $l_s > 10$ nm [7]. Inelastic neutron scattering experiments on phonons in LSCO also show an anomaly with a characteristic wave vector $k_0 \sim \pi/2a$ (where a is the lattice constant), corresponding to a length scale of the underlying textures of $l \approx 2$ nm [5]. Comparing these values with l_e and l_m in Fig. 3(a), albeit for the limited data that exist, we see impressive agreement, suggesting that the structural coherence length l_s corresponds closely with the characteristic electronic inhomogeneity length scale l_e.

An interesting question is whether the behavior $l_e \rightarrow \xi_s(0)$, as $T \rightarrow T_c$ is evident also for n-type materials such as $Nd_{2-x}Ce_xCuO_4$ (NCCO) [14], even though $\xi_s(0)$ is approximately an order of magnitude larger than in p-type cuprate [24]. In Fig. 3(b) we compare the normalized phonon escape length $l_e/\xi_s(0)$ vs T/T_c for optimally doped LSCO and NCCO (both $x = 0.15$). Remarkably, the normalized $l_e/\xi_s(0)$ is very similar for NCCO and LSCO over a substantial temperature range near and above T_c.

In contrast to the behavior above and near T_c, the T dependence of l_e *well below* T_c does not appear to be universal. For example, τ_r (and hence also l_e) has previously been suggested to follow power law behavior of the form $\tau_r \sim T^{-\eta}$ with $\nu = 3$ below T_c in LSCO [15], but this is apparently not always the case, as we can see from Fig. 3.

Expressing the escape length as $l_e/\xi_s(0) = (T/T_c)^{-\eta}$, in Fig. 3(b) we observe very different behavior in LSCO and NCCO, with $\eta \approx 2$ and $\nu \approx 0$, respectively. Furthermore, an examination of data for τ_r on $YBa_2Cu_3O_{7-\delta}$ [12], $Bi_2Sr_2CaCu_2O_8$ [12], and $HgBa_2Ca_2Cu_3O_8$ [16] also reveals quite diverse behavior below T_c, which might be an indication that the typical T dependence of l_e may not be intrinsic but is determined by characteristic lattice defect textures or impurities. In fact, the T dependence of τ_r in high quality underdoped single crystals of $YBa_2Cu_3O_{6.5}$ [25] shows markedly different T dependence than in

quenched thin film samples (presumably with quenched O disorder) [11,12], the former showing much longer relaxation times (and hence longer l_e) below T_c, highlighting the importance of disorder, domains, and defects. Indeed, well below T_c, as the relaxation time τ_r increases, competing relaxation processes may become operative. Unfortunately, without comparisons with other experimental data, we cannot empirically justify the steady-state assumption in Eqs. (1) and (2) as we did for $T \geq T_c$, and we presently refrain from further analysis of τ_r only in terms of Eq. (3) well below T_c. Although we have concentrated here on LSCO, from published data for τ_r and $\sigma(T)$ for $YBa_2Cu_3O_{7-\delta}$ [12], $Bi_2Sr_2CaCu_2O_8$ [12], and $HgBa_2Ca_2Cu_3O_8$ [16] and comparison of l_e, l_m, and l_s, we can deduce that, qualitatively, the behavior is common, particularly (i) $l_e(T) \approx \xi_s(0)$ above T_c (but below T^*) and (ii) the divergence of $l_e(T)$ around T_c.

In the interest of brevity, in this Letter we have oversimplified a number of issues, particularly the importance of the anisotropy of l_e. In spite of this, the present analysis makes it clear that the physical properties of cuprates may be expected to be dominated by inhomogeneity, with different length scales at different T and x.

To conclude, we suggest a physical picture which can lead to the observed behavior of l_e. Doped holes are unbound at high temperature, but at some temperature T^*—associated with the energy scale $kT^* \sim 2\Delta$, where Δ is the binding energy per particle—they start to form bound bipolaron pairs, leading to a charge-inhomogeneous state. These objects form and dissociate according to thermal fluctuations, leading to a state which is dynamically inhomogeneous. The dimensions of these objects are determined by the balance of Coulomb repulsion and lattice attraction, as discussed in Ref. [27], for example, and is of the order of the coherence length, $l = 1$–2 nm above T_c. As the temperature is reduced and the density of pairs increases, these pairs start to coalesce into larger objects, which is reflected by the longer length scale l_e at low temperatures [28]. At some critical temperature T_c, the characteristic length scale becomes comparable to the superconducting coherence length $l(T) \approx \xi_{GL}(T)$, the percolation threshold is reached, and a macroscopically phase-coherent state is established [20].

The author wishes to thank V. V. Kabanov and J. Demsar for valuable discussions and suggestions, P. Kusar and J. Demsar for supplying the raw data on LSCO, and S. Sugai for kindly supplying the single crystals on which the analysis is based.

[1] See, for example, special issues 1 and 2 of the Proceedings of the International Conference on Dynamic Inhomogeneities in Complex Oxides, edited by K. A. Müller, D. Mihailovic, and A. Bussmann-Holder [J. Supercond. **17**, 1 (2004)]; D. Mihailovic and K. A. Müller, *High-Tc Superconductivity 1996: Ten Years after the Discovery*, NATO ASI, Ser. E, Vol. 343 (Kluwer, Dordrecht, 1997), p. 243; A. R. Bishop *et al.*, J. Phys. Condens. Matter **15**, L169 (2003).

[2] See, for example, A. Bianconi *et al.*, Phys. Rev. Lett. **76**, 3412 (1996); M. Acosta-Alejandro *et al.*, J. Supercond. **15**, 355 (2002), and references therein.

[3] E. S. Bozin *et al.*, Physica (Amsterdam) **341C**, 1793 (2000); E. S. Bozin *et al.*, Phys. Rev. Lett. **84**, 5856 (2000).

[4] T. Egami and S. Billinge, *Underneath the Bragg Peaks: Structural Analysis of Complex Materials* (Pergamon, New York, 2003).

[5] R. J. McQueeney *et al.*, Phys. Rev. Lett. **82**, 628 (1999).

[6] Z. Islam *et al.*, Phys. Rev. B **66**, 092501 (2002).

[7] H. Kimura *et al.*, J. Phys. Soc. Jpn. **69**, 851 (2000).

[8] D. J. Derro *et al.*, Phys. Rev. Lett. **88**, 97 002 (2002); S. H. Pan *et al.*, Nature (London) **413**, 282 (2001); C. Howald *et al.*, Phys. Rev. B **67**, 014533 (2003); K. McElroy *et al.*, Nature (London) **422**, 592 (2003).

[9] A. Rothwarf and B. N. Taylor, Phys. Rev. Lett. **19**, 27 (1967).

[10] G. A. Sai-Halasz *et al.*, Phys. Rev. Lett. **33**, 215 (1974); J. L. Levine and S. Y. Hsieh, Phys. Rev. Lett. **20**, 994 (1968); S. B. Kaplan *et al.*, Phys. Rev. B **14**, 4854 (1976).

[11] V. V. Kabanov *et al.*, Phys. Rev. B **59**, 1497 (1999).

[12] S. G. Han *et al.*, Phys. Rev. Lett. **65**, 2708 (1990); C. J. Stevens *et al.*, Phys. Rev. Lett. **78**, 2212 (1997); G. L. Easley *et al.*, Phys. Rev. Lett. **65**, 3445 (1990); D. C. Smith *et al.*, Physica (Amsterdam) **341C**, 2219 (2000); **341C**, 2221 (2000); P. Gay *et al.*, J. Low Temp. Phys. **117**, 1025 (1999).

[13] J. Demsar *et al.*, Phys. Rev. Lett. **83**, 800 (1999).

[14] Y. Liu *et al.*, Appl. Phys. Lett. **63**, 979 (1993).

[15] S. Rast *et al.*, Phys. Rev. B **64**, 214505 (2001).

[16] J. Demsar *et al.*, Phys. Rev. B **63**, 54 519 (2001).

[17] G. Bianchi, C. Chen, and J. F. Ryan, J. Low Temp. Phys. **131**, 755 (2003).

[18] P. Kusar, J. Demsar, V. V. Kabanov, S. Sugai, and D. Mihailovic (unpublished).

[19] Y. S. He *et al.*, Physica (Amsterdam) **165B**, 1283 (1990).

[20] D. Mihailovic, V. V. Kabanov, and K. A. Müller, Europhys. Lett. **57**, 254 (2002).

[21] V. G. Grebenik *et al.*, Hyperfine Interact. **61**, 1093 (1990).

[22] X. J. Zhou *et al.*, Nature (London) **423**, 398 (2003).

[23] H. Takagi *et al.*, Phys. Rev. Lett. **69**, 2975 (1992).

[24] G. I. Harus *et al.*, cond-mat/9912004.

[25] G. P. Segre *et al.*, Phys. Rev. Lett. **88**, 137001 (2002).

[26] D. Mihailovic and V. V. Kabanov, J. Supercond. **17**, 21 (2004).

[27] D. Mihailovic and V. V. Kabanov, Phys. Rev. B **63**, 054505 (2001); V. V. Kabanov and D. Mihailovic, J. Supercond. **13**, 959 (2000); Phys. Rev. B **65**, 212508 (2002).

[28] V. V. Kabanov, T. Mertelj, and D. Mihailovic (unpublished).

[29] M. Hase *et al.*, Physica (Amsterdam) **185C–189C**, 1855 (1991).

[30] I. G. Kolobov *et al.*, Phys. Rev. B **49**, 744 (1994).